Can a Driver Assistance System Determine if a Driver is Perceiving a Pedestrian?
Consideration of the Driver's Visual Adaptation to Illumination Change

Yuki Imaeda[1], Takatsugu Hirayama[1], Yasutomo Kawanishi[1],
Daisuke Deguchi[2], Ichiro Ide[1] and Hiroshi Murase[1]

[1]*Graduate School of Information Science, Nagoya University, Furo-cho, Chikusa-ku, Nagoya-shi, Aichi, Japan*
[2]*Information Strategy Office, Nagoya University, Furo-cho, Chikusa-ku, Nagoya-shi, Aichi, Japan*
imaeday@murase.m.is.nagoya-u.ac.jp, {hirayama, kawanishi}@is.nagoya-u.ac.jp,
ddeguchi@nagoya-u.jp,{ide, murase}@is.nagoya-u.ac.jp

Keywords: ITS, Driving Assistance, Detectability, Ambient Light, Visual Adaptation.

Abstract: We propose an estimation method of pedestrian detectability considering the driver's visual adaptation to illumination change. Since it is important for driver assistance systems to determine if a driver is perceiving a pedestrian or not, estimation of pedestrian detectability by the driver is required. However, previous studies do not consider drastic illumination changes that degrades the detection performance by the driver. We assumed that driver's visual characteristics change in proportion to the adaptation period after illumination change. Therefore we constructed estimators corresponding to different adaptation periods, and estimated the pedestrian detectability by switching them according to the period. To evaluate the proposed method, we constructed an experimental environment to present a subject with illumination changes and conducted an experiment to measure and estimate the pedestrian detectability according to the adaptation period. Results showed that the proposed method could estimate the pedestrian detectability accurately after the illumination changed drastically.

1 INTRODUCTION

The number of road traffic deaths was 1.25 million globally in 2013, which has not decreased since 2007 (World Health Organization, 2015). Particularly, the number of pedestrian deaths was about 280 thousand. Also, the proportion of accidents caused by driver's negligence was over 90% (NHTSA's National Center for Statistics and Analysis, 2015). The factors in the negligence can be classified into recognition, decision, operation, and other errors (sleeping, etc.). Among them, the recognition error was the major factor. So assisting the drivers with pedestrian recognition is important for the reduction of accidents.

Recently, various methods for pedestrian detection have been proposed (Viola et al., 2005; Rohling et al., 2010). Automobile manufacturers have started to apply them for Advanced Driving Assistance Systems which warn a driver to pay attention to pedestrians or automatically avoid them. On the other hand, over-intervention in driving can impede safe driving rather than help that. The systems, therefore, should estimate the pedestrian detectability by the driver and make him/her pay attention to pedestrians only with low detectability.

The pedestrian detectability is defined as the probability of perceiving a pedestrian by the driver (Engel and Curio, 2012). Factors that change the pedestrian detectability are classified into pedestrian's appearance, driver's condition, and traffic environment. The appearance factor the contains pedestrian's shape, color, motion, and so on. There are some studies on pedestrian detectability estimation focusing on his/her appearance (Wakayama et al., 2012; Tanishige et al., 2014). The driver's condition factor contains fatigue, distraction, and declining with advancing age. Wegner et al. indicated that driver's visual performance declines also in intoxicated states (Wegner and Fahle, 1999). The traffic environment factor contains road condition, weather, time, and so on. Arumi et al. showed that visual acuity worsens according to the road luminance level (Arumi et al., 1997).

In this paper, we focus on drastic illumination change in the traffic environment, especially bright-to-dark change, as a critical factor of road traffic ac-
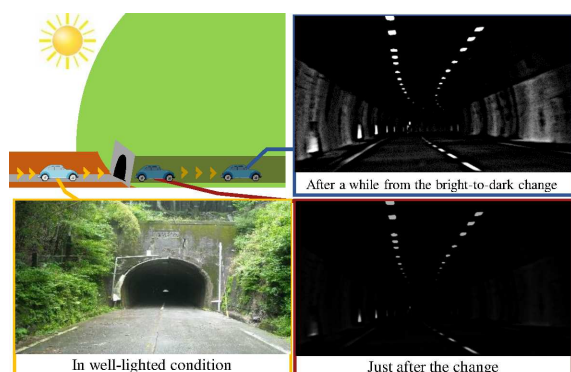
611

Figure 1: Simulation example of driver's vision after bright-to-dark illumination change.

Figure 2: Process flow of the proposed framework.

cidents. To the best of our knowledge, this has not been considered in previous works on the estimation of pedestrian detectability. Figure 1 shows a simulation example of a driver's vision after the bright-to-dark illumination change. After the change, the driver's visual acuity decreases during the adaptation period until adapting to the dark illumination (Dark adaptation). Studies on dark adaptation in the field of psychophysics is performed by two visual functions; "Pupillary light reflex" and "Purkinje phenomenon." From previous research (Rushton, 1961), it is known that the former lasts for several seconds, while the latter lasts for a few minutes. It implies that the change affects the driver's visual characteristics for a while although he/she needs to response rapidly. However, it might be difficult to apply the insights from such studies to pedestrian detectability estimation, since they used simple visual stimulate such as Gabor patches and LED lights for measuring visual sensitivity, while drivers are exposed to more complex visual stimulate in real driving conditions.

The goal of our research is to estimate the pedestrian detectability correctly even after the illumination changes drastically. The pedestrian detectability depends on environmental variables (e.g., contrast of luminance, visual adaptation period), and individual internal variables of a driver (e.g., eye sight, age). In this paper, we focus on the visual adaptation period since it is the most direct measure of a temporal effect to the driver's visual characteristics. After illumination changes drastically, a driver's visual characteristics change according to the adaptation period. So, we propose a detectability estimation method considering visual adaptation to drastic illumination changes. The method constructs several estimators and estimate the pedestrian detectability by switching them according to the adaptation period. In summary, our contributions are as follows:
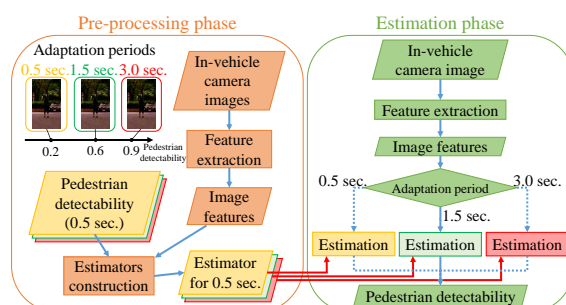
1. Introduction of driver's visual adaptation: By

switching estimators according to the adaptation period, the accuracy of the pedestrian detectability estimation increases.

2. Dataset construction of the pedestrian detectability with illumination changes: We design an experimental procedure to obtain the pedestrian detectability with visual adaptation.

2 DETECTABILITY ESTIMATION

As mentioned in Section 1, after the illumination changes drastically, the driver's visual characteristics change according to the adaptation period. So, the proposed method estimates the pedestrian detectability by switching estimators according to the adaptation period. Figure 2 shows the process flow of the proposed framework. It consists of two phases; pre-processing phase, and estimation phase.

In the pre-processing phase, detectability estimators are trained by using pairs of features and the ground-truth of the detectability. For each adaptation period, the ground-truth is obtained through a preliminary experiment and the estimator is trained. The estimators are constructed by Support Vector Regression. In Figure 2, the adaptation period is set to either 0.5, 1.5, or 3.0 sec.

In the estimation phase, we first measure the driver's gaze position and extract visual features from an in-vehicle camera image. Then, pedestrian detectability is estimated by using the estimators trained in the pre-processing phase. To estimate considering the driver's visual adaptation, first, drastic illumination change points are detected using an illuminometer. We defined the time after the change as the driver's visual adaptation period, and switch estimators according to certain periods and estimate the detectability at each period.

Feature Extraction. We apply features used in a conventional method (Tanishige et al., 2014) for the

Table 1: List of features.

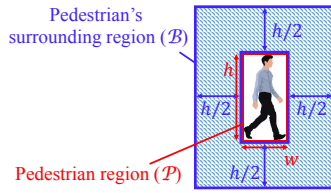| Abbr.	Description
P_{width}	Width of pedestrian region
P_{height}	Height of pedestrian region
$P_{\delta(\text{lum})}$	Standard deviation of luminance
$C_{\mu(\text{lum})}$	Contrast of luminance
$C_{\mu(\text{Lab})}$	Contrast of average color (L*a*b*)
C_{edge}	Contrast of edge
$C_{\text{hist(color)}}$	Contrast of color histogram
$D_{(p,g)}$	Distance between center of the pedestrian region and fixation point

Figure 3: Pedestrian region and its surrounding region.

detectability estimation. Table 1 shows the list of features used. Here, the pedestrian region $\mathcal{P}$ and its surrounding region $\mathcal{B}$ are defined as shown in Figure 3.

Features from the Pedestrian Region. In general, the larger a pedestrian appears, and the more complex the texture of the pedestrian region is, the easier the driver can detect. We assume that these visual characteristics influence the detectability even after a drastic illumination change. Therefore, we extract features related to the size of a pedestrian and its texture.

P_{width} and P_{height} are the width and the height of the pedestrian region, respectively; w and h in Figure 3.

$P_{\sigma(\text{lum})}$ is the standard deviation of luminance in the pedestrian region. First, we convert an input image to an 8-bit grey scale image and calculate the average of luminance in the pedestrian region as

$$\bar{l}_{\mathcal{P}} = \frac{1}{|\mathcal{P}|} \sum_{(i,j)\in\mathcal{P}} l(i,j), \qquad (1)$$

where $|\mathcal{P}|$ represents the number of pixels in region $\mathcal{P}$, and $l(i,j)$ represents the luminance at pixel (i,j). Then, the standard deviation $P_{\sigma(\text{lum})}$ is calculated as

$$P_{\sigma(\text{lum})} = \sqrt{\frac{1}{wh}\sum_{i=1}^{w}\sum_{j=1}^{h}(l(i,j)-\bar{l}_{\mathcal{P}})^2}. \qquad (2)$$

Features of the Contrast between the Appearances of Pedestrian Region and Its Surrounding Region. The contrast between the appearances of a pedestrian and its surrounding (background) is an important feature considering pedestrian detectability.

$C_{\mu(\text{lum})}$ is the contrast between the average luminance in the pedestrian region and that in the sur-

rounding region. We first calculate the average luminance in the surrounding region $\bar{l}_{\mathcal{B}}$ as with Equation (1). Then, $C_{\mu(\text{lum})}$ is calculated as

$$C_{\mu(\text{lum})} = \left|\bar{l}_{\mathcal{P}} - \bar{l}_{\mathcal{B}}\right|, \qquad (3)$$

where $|\cdot|$ represents the absolute value.

$C_{\mu(\text{Lab})}$ is the contrast between the average color in the pedestrian region and that in its surrounding region. First, we calculate the average color in the pedestrian region $\bar{v}_{\mathcal{P}}$, and that in its surrounding region $\bar{v}_{\mathcal{B}}$, as

$$\bar{v}_{\mathcal{P}} = \frac{1}{|\mathcal{P}|} \sum_{(i,j)\in\mathcal{P}} v(i,j), \qquad (4)$$

$$\bar{v}_{\mathcal{B}} = \frac{1}{|\mathcal{B}|} \sum_{(i,j)\in\mathcal{B}} v(i,j), \qquad (5)$$

where $v(i,j)$ is a vector in the L*a*b* color space. Then, $C_{\mu(\text{Lab})}$ is calculated as

$$C_{\mu(\text{Lab})} = \sqrt{\|\bar{v}_{\mathcal{P}} - \bar{v}_{\mathcal{B}}\|^2}, \qquad (6)$$

where $\|\cdot\|$ represents the Euclidean norm.

C_{edge} is the contrast between the average of edge intensity in the pedestrian region and that in its surrounding region. First, Sobel filter is applied to the grey scale image to obtain an edge intensity image. Then, the average edge intensity is calculated in the pedestrian region $\bar{E}_{\mathcal{P}}$, and that in its surrounding region $\bar{E}_{\mathcal{B}}$, as

$$\bar{E}_{\mathcal{P}} = \frac{1}{|\mathcal{P}|} \sum_{(i,j)\in\mathcal{P}} E(i,j), \qquad (7)$$

$$\bar{E}_{\mathcal{B}} = \frac{1}{|\mathcal{B}|} \sum_{(i,j)\in\mathcal{B}} E(i,j), \qquad (8)$$

where $E(i,j)$ is the edge intensity at pixel (i,j). Finally, C_{edge} is calculated as

$$C_{\text{edge}} = \left|\bar{E}_{\mathcal{P}} - \bar{E}_{\mathcal{B}}\right|. \qquad (9)$$

$C_{\text{hist(color)}}$ is the contrast between the color histogram in the pedestrian region $H_{\text{RGB}}(\mathcal{P})$, and that in its surrounding region $H_{\text{RGB}}(\mathcal{B})$, which are generated by combining 16-bins histograms from the R, G, and B values. Then, $C_{\text{hist(color)}}$ is calculated as

$$C_{\text{hist(color)}} = d_{\text{EMD}}(H_{\text{RGB}}(\mathcal{P}), H_{\text{RGB}}(\mathcal{B})), \qquad (10)$$

where $d_{\text{EMD}}(H_1, H_2)$ represents the Earth Mover's Distance (Rubner et al., 1998).

Distance from a Pedestrian Region to the Driver's Gaze Position. According to psychophysics studies, the visual adaptation in the central fields-of-view differs from that in the peripheral fields-of-view. Therefore, we focus on the view angle from the pedestrian to the driver's gaze position. The Euclidean distance between the center of the pedestrian region and the fixation point on an input image is represented as $D_{(p,g)}$.
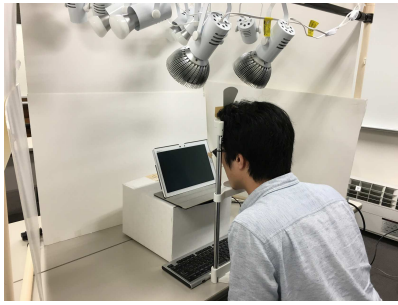
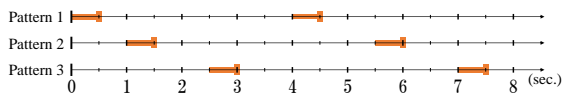Figure 4: Experimental facility (Covered with a blackout curtain during the actual subjective experiment).

Figure 5: Patterns of display timings of images after the light is turned off at 0 sec. The orange horizontal bar indicates the duration of displaying the image, where we obtain the detectability.

3 DATASET CONSTRUCTION

The pedestrian detectability is the probability that a driver perceives a pedestrian (Engel and Curio, 2012). Since this is the measure based on human sensation, we need to conduct a subjective experiment to obtain the ground-truth before training the estimators. Some works regarded the rate of detecting a pedestrian by human subjects as the detectability (Wakayama et al., 2012; Tanishige et al., 2014). They asked the subjects to find a pedestrian in an image capturing a traffic scene in stable illumination condition. Since we focus on the visual adaptation period, we designed an experimental environment to change the illumination at an arbitrary timing. Figure 4 shows the facility with controllable lights to realize the environment. During the experiment, we covered the facility and the subject with a blackout curtain to shut out external light. The procedure is described below.

1. The subject adapts to well-lighted environment in the facility for 30 sec.

2. A low-resolution image capturing a traffic scene including a non-detectable pedestrian is displayed to the subject.

3. The subject is instructed to fix his/her eye gaze at a certain position indicated by a cross.

4. The illumination is drastically changed by turning off the lights.

5. After T [sec.], a high-resolution image of the same scene as Step 2. is displayed for 0.5 sec.

6. The subject searches the pedestrian in the image.

Figure 6: Examples of images in the dataset.

7. The subject indicates the position of the pedestrian by touching the display.

8. The cross is displayed again, then Steps 2. to 7. except for Step 4., are repeated once more with another image.

We displayed the low-resolution image of the same scene as the high-resolution image to reduce the effect of visual surprise. We conducted the procedure with T = 0.0, 1.0, 2.5, 4.0, 5.5, and 7.0 sec. For efficiency of time, we displayed two scenes (the first one with, and the second one without illumination change) in a single procedure. Hence, we obtained the detectability corresponding to six adaptation periods by carrying out the procedure with three patterns of display timings of images as shown in Figure 5. In addition, we fixed the luminance in the well-lit environment to about 1,000 luxes, that is, the luminance at an hour before sunset, and that in the dark environment with about 10 luxes to reproduce twilight gloom.

We used a camera (iVIS HF G10, Canon Inc.) to capture traffic scenes in twilight. Then we manually extracted frames containing one pedestrian from the videos. Figure 6 shows four examples of images whose resolution is 1,920 × 1,080 pixels. We also used an organic electroluminescent display (arrows Tab F-03G, Fujitsu Inc., 10.5 inches, 2,560 × 1,600 pixels, 2,000,000:1 contrast ratio) with touch panel to display the images, and some lights (Grassy LeDiO RX122 FleshWhite, Volxjapan Co. Ltd. and Hue, Philips) to control the illumination condition.

Figure 7 shows a criterion to judge whether the subject's response is correct or not. We defined a center region of the pedestrian region as ground-truth, and a 200 pixels[1] square around the touched point as the response region. If it overlapped with the ground-truth, it was regarded as correct. Then we calculated the rate of correct responses by all subjects as the pedestrian detectability.

We conducted this experiment with four subjects (three males and one female) with normal vision

---

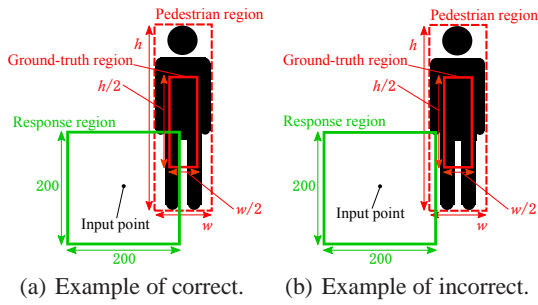[1]Corresponds to about five degs. in the visual field.

Figure 7: Criterion for the judgement of the subject's response.

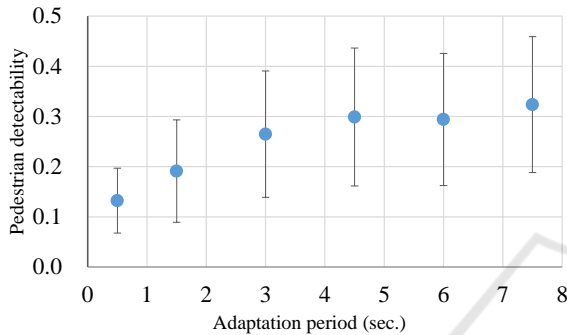(a) Example of correct. (b) Example of incorrect.

Figure 8: Relation between the pedestrian detectability and the adaptation period.

Figure 9: Distribution of the pedestrian detectability for each adaptation period.

Table 2: Evaluation result.

Adaptation period	Mean Squared Error	
	Proposed	Comparative
0.5 sec.	0.069	0.066
1.5 sec.	0.108	0.110
3.0 sec.	0.134	0.144
4.5 sec.	0.144	0.177
6.0 sec.	0.140	0.169
7.5 sec.	0.141	0.185
Avg.	0.123	0.134

(Rushton, 1961). We therefore infer that this result reflected the visual recovery of the former.

Figure 9 shows the distributions of the pedestrian detectability for each adaptation period. This result indicates that the longer the adaptation period is, the less the number of pedestrians which has zero detectability is.

4 RESULT AND DISCUSSION

To construct the multiple estimators for the proposed method, we divided the dataset into six groups according to the adaptation periods and trained six estimators using each group. To evaluate the proposed method considering the visual adaptation, we compared the estimation error with a comparative method which used a single estimator trained with all of the detectability data, in a similar way to previous studies (Engel and Curio, 2012; Wakayama et al., 2012). Leave-one-pedestrian-out cross validation was applied that is 50 pedestrians were used for training and one pedestrian for testing.

Table 2 shows the comparison of the estimation error for each adaptation period between the proposed method and the comparative method. The estimation errors in which the adaptation period was 0.5 and 1.5 sec. were low for both methods. On the other hand, focusing on the longer 3.0 sec., the proposed method had lower error than the comparative method. The estimators might have overfit to the dataset because it had a large bias in the detectability distribution for which the adaptation period was 0.5 and 1.5 sec.

For discussion, we analyzed the effectiveness of the features for each adaptation period. In detail, we first chose a couple of features from the eight visual features, then constructed estimators corresponding to the adaptation period and evaluated them. This procedure was applied to all combinations of features ($_8C_2 = 28$). Finally we placed them in ascending order of the estimation error.

Table 3 shows the order and Mean Squared Er-

whose ages ranged between 22 and 30. In this experiment, we prepared 51 images containing just one pedestrian in each of them. Thus we obtained 306 ground-truth data, i.e., 51 pedestrians for each of six adaptation periods, of the pedestrian detectability.

Figure 8 shows the relation between the obtained pedestrian detectability and the adaptation period. Here, the points and lines represent the average and variance of the pedestrian detectability of 51 pedestrians, respectively. From this result, we can say that the pedestrian detectability increased gradually until 4.5 sec. in this experiment. As mentioned in Section 1, the dark adaptation is performed by the following two visual functions; "Pupillary light reflex" and "Purkinje phenomenon." The former lasts for several seconds, while the latter lasts for a few minutes

Table 3: Order of the pair of image features (Evaluated by Mean Squared Error).

Order	Adaptation period					
	0.5 sec.	1.5 sec.	3.0 sec.	4.5 sec.	6.0 sec.	7.5 sec.
1	$P_{\delta(\text{lum})}, C_{\text{edge}}$ 0.047	$C_{\mu(\text{Lab})}, C_{\text{edge}}$ 0.060	$P_{\delta(\text{lum})}, C_{\mu(\text{lum})}$ 0.063	$P_{\delta(\text{lum})}, C_{\mu(\text{lum})}$ 0.084	$P_{\delta(\text{lum})}, C_{\mu(\text{lum})}$ 0.081	$P_{\delta(\text{lum})}, C_{\mu(\text{lum})}$ 0.059
2	$P_{\delta(\text{lum})}, C_{\mu(\text{lum})}$ 0.052	$P_{\delta(\text{lum})}, C_{\text{edge}}$ 0.061	$P_{\delta(\text{lum})}, C_{\mu(\text{Lab})}$ 0.067	$P_{\text{height}}, C_{\mu(\text{Lab})}$ 0.103	$P_{\delta(\text{lum})}, C_{\mu(\text{Lab})}$ 0.087	$P_{\delta(\text{lum})}, C_{\mu(\text{Lab})}$ 0.083
3	$P_{\text{width}}, C_{\text{edge}}$ 0.059	$P_{\delta(\text{lum})}, C_{\mu(\text{Lab})}$ 0.069	$P_{\text{width}}, C_{\text{edge}}$ 0.071	$P_{\delta(\text{lum})}, C_{\mu(\text{Lab})}$ 0.106	$P_{\text{height}}, C_{\mu(\text{Lab})}$ 0.107	$P_{\text{width}}, C_{\text{edge}}$ 0.104

ror of each combination. This result indicates that after 3.0 sec., $C_{\mu(\text{lum})}$ and $C_{\mu(\text{Lab})}$ contributed to achieve lower estimation error. On the other hand, just after 0.5 and 1.5 sec., C_{edge} contributed. This also indicates that the same combinations achieved low error after 3.0 sec. Hence it is inferred that after 3.0 sec., the change of visual characteristic would be small.

5 CONCLUSION

In this paper, we proposed a method for the estimation of pedestrian detectability considering visual adaptation to drastic illumination changes, and indicated that a driver assistance system can determine if a driver is perceiving a pedestrian to some extent. Specifically, the proposed method extracts visual features and estimates the pedestrian detectability by switching the estimators according to the adaptation period.

To evaluate the proposed method, we first constructed an experimental environment to present a subject with drastic illumination changes and then conducted an experiment to measure and estimate the pedestrian detectability according to different adaptation periods. Evaluation results showed that the proposed method considering the visual adaptation was effective for the estimation of the pedestrian detectability. In addition, we analyzed the effective features for each adaptation period.

In future work, we will introduce additional features based on physiological knowledge, and conduct subjective experiments to expand the dataset. Furthermore, we will apply the obtained knowledge to an actual vechicle to validate the application possibility.

ACKNOWLEDGEMENTS

REFERENCES

Arumi, P., Chauhan, K., and Charmant, W. (1997). Accommodation and acuity under night-driving illumination levels. *Ophthalmic and Physiological Optics*, 17(4):291–299.

Engel, D. and Curio, C. (2012). Detectability prediction in dynamic scenes for enhanced environment perception. In *Proc. 2012 IEEE Intelligent Vehicles Symposium*, pages 178–183.

NHTSA's National Center for Statistics and Analysis (2015). Critical reasons for crashes investigated in the national motor vehicle crash causation survey.

Rohling, H., Heuel, S., and Ritter, H. (2010). Pedestrian detection procedure integrated into an 24 ghz automotive radar. In *Proc. 2010 IEEE Radar Conf.*, pages 1229–1232.

Rubner, Y., Tomasi, C., and Guibas, L. J. (1998). A metric for distributions with applications to image databases. In *Proc. 6th Int. Conf. on Computer Vision*, pages 59–66.

Rushton, W. A. H. (1961). Rhodopsin measurement and dark-adaptation in a subject deficient in cone vision. *J. Physiology*, 156(1):193–205.

Tanishige, R., Deguchi, D., Doman, K., Mekada, Y., Ide, I., and Murase, H. (2014). Prediction of driver's pedestrian detectability by image processing adaptive to visual fields of view. In *Proc. 17th IEEE Int. Conf. on Intelligent Transportation Systems*, pages 1388–1393.

Viola, P., Jones, M. J., and Snow, D. (2005). Detecting pedestrians using patterns of motion and appearance. *Int. J. of Computer Vision*, 63(2):153–161.

Wakayama, M., Deguchi, D., Doman, K., Ide, I., Murase, H., and Tamatsu, Y. (2012). Estimation of the human performance for pedestrian detectability based on visual search and motion features. In *Proc. 21st IAPR Int. Conf. on Pattern Recognition*, pages 1940–1943.

Wegner, A. J. and Fahle, M. (1999). Alcohol and visual performance. *Progress in Neuro-Psychopharmacology and Biological Psychiatry*, 23(3):465–482.

World Health Organization (2015). Global status report on road safety 2015.